Final Report (AOARD-05-4015)

Structural Optimization Using the Equivalent Static Load Concept

Gyung-Jin Park

Professor
Department of Mechanical Engineering
Hanyang University
1271 Sa-1 Dong, Sangnok-gu, Ansan City,
Gyeonggi-do 426-791, Korea

November 2005

Report Documentation Page

Form Approved
OMB No. 0704-0188

1. REPORT DATE	2. REPORT TYPE	3. DATES COVERED
27 JUL 2006	**Final Report (Technical)**	**28-10-2004 to 28-02-2006**

4. TITLE AND SUBTITLE
Structural Optimization Using the Equivalent Load Concept

5a. CONTRACT NUMBER
FA520905P0085

5b. GRANT NUMBER

5c. PROGRAM ELEMENT NUMBER

6. AUTHOR(S)
Gyung-Jin Park

5d. PROJECT NUMBER

5e. TASK NUMBER

5f. WORK UNIT NUMBER

7. PERFORMING ORGANIZATION NAME(S) AND ADDRESS(ES)
Hanyang University,Sa-Dong, Ansan,,Kyunggi-Do 425-170,KOREA,KE,425-170

8. PERFORMING ORGANIZATION REPORT NUMBER
AOARD-054015

9. SPONSORING/MONITORING AGENCY NAME(S) AND ADDRESS(ES)
The US Resarch Labolatory, AOARD/AFOSR, Unit 45002, APO, AP, 96337-5002

10. SPONSOR/MONITOR'S ACRONYM(S)
AOARD/AFOSR

11. SPONSOR/MONITOR'S REPORT NUMBER(S)
AOARD-054015

12. DISTRIBUTION/AVAILABILITY STATEMENT
Approved for public release; distribution unlimited

13. SUPPLEMENTARY NOTES

14. ABSTRACT
The joined-wing is a new concept of the airplane wing. The fore-wing and the aft-wing are joined together in a joined-wing. The range and loiter are longer than those of a conventional wing. The joined-wing can lead to increased aerodynamic performance and reduction of the structural weight. In this research, dynamic response optimization of a joined-wing is carried out by using equivalent static loads. Equivalent static loads are made to generate the same displacement field as the one from dynamic loads at each time step of dynamic analysis. The gust loads are considered as critical loading conditions and they dynamically act on the structure of the aircraft. It is difficult to identify the exact gust load profile. Therefore, the dynamic loads are assumed to be (1-cosine) function. Static response optimization is performed for the two cases. One uses the same design variable definition as dynamic response optimization. The other uses the thicknesses of all elements as design variables.

15. SUBJECT TERMS
Optimization

16. SECURITY CLASSIFICATION OF:			17. LIMITATION OF ABSTRACT	18. NUMBER OF PAGES	19a. NAME OF RESPONSIBLE PERSON
a. REPORT	b. ABSTRACT	c. THIS PAGE			
unclassified	**unclassified**	**unclassified**		**41**	

Abstract

The joined-wing is a new concept of the airplane wing. The fore-wing and the aft-wing are joined together in a joined-wing. The range and loiter are longer than those of a conventional wing. The joined-wing can lead to increased aerodynamic performance and reduction of the structural weight. In this research, dynamic response optimization of a joined-wing is carried out by using equivalent static loads. Equivalent static loads are made to generate the same displacement field as the one from dynamic loads at each time step of dynamic analysis. The gust loads are considered as critical loading conditions and they dynamically act on the structure of the aircraft. It is difficult to identify the exact gust load profile. Therefore, the dynamic loads are assumed to be (1-cosine) function. Static response optimization is performed for the two cases. One uses the same design variable definition as dynamic response optimization. The other uses the thicknesses of all elements as design variables. The results are compared.

Table of Contents

LIST OF FIGURES

LIST OF TABLES

1 Introduction

The joined-wing has the advantage of a longer range and loiter than of a conventional wing. First, Wolkovich published the joined-wing concept in 1986. [1] Gallman and Kroo offered many recommendations for the design methodology of a joined-wing. [2] They used the fully stressed design (FSD) for optimization. Blair and Canfield initiated nonlinear exploration on a joined-wing configuration in 2005. [3] Air Force Research Laboratories (AFRL) have been developing an airplane with the joined-wing to complete a long-endurance surveillance mission. [4-7] Figure 1 shows a general joined-wing aircraft. An airplane with a joined-wing may be defined as an airplane that has diamond shapes in both top and front views. The fore-wing and aft-wing are joined in the joined-wing.

Real loads during flight are dynamic loads. But it is difficult to evaluate exact dynamic loads. Also, dynamic response optimization, which uses dynamic loads directly, is fairly difficult. When the dynamic loads are directly used, there are many time dependent constraints and the peaks are changed when the design is changed. Since special treatments are required, the technology is rarely applied to large-scale structures. [8] Instead, static response optimization is carried out. Therefore, static loads, which approximate dynamic loads, have been used in structural optimization of the joined-wing. However, there are many problems in existing transformation methods. For example,

dynamic loads are often transformed to static loads by multiplying the dynamic factors to the peak of the dynamic loads. But this method does not consider the vibration or inertia properties of the structure. The equivalent static loads are used to overcome these difficulties. The method using equivalent static loads has been proposed by Choi and Park. [9] The equivalent static load is defined as a static load which generates the same displacement field as that under a dynamic load. The load is made at each time step of dynamic analysis. The loads are utilized as multiple loading conditions in structural optimization. [8-16]

Size optimization is performed to reduce the structural mass while design conditions are satisfied. Existing static loading conditions are utilized. Since the condition for the gust load has the most dynamic effect, only the gust loads among the existing static loads are transformed to dynamic loads. Dynamic gust loads are calculated by multiplying static loads by the (1-cosine) function. Then, a coefficient is defined in order to make the peak of the dynamic load the same as the displacement under the static gust load. The calculated dynamic load is transformed to equivalent static loads for static response optimization. As boundary conditions of the finite element model, the fore-wing root parts are fixed and the aft-wing root parts are enforced to have certain displacements to maintain stability during flight. NASTRAN and GENESIS are used for size optimization. [17-18] Results from dynamic response optimization using equivalent static loads and static response optimization are compared.

2 Structural optimization under equivalent static loads

Dynamic loads are real forces which change in the time domain while static loads are ideal forces which are constant regardless of time. Structures under dynamic loads vibrate and this behavior cannot be represented by the static loads. There are various methods to transform the dynamic loads into static loads. One method of transformation is the equivalent static load method. In structural optimization, the equivalent static loads include the dynamic effects very well.

2.1 Transformation of dynamic loads into equivalent static loads

An equivalent static load is defined as a static load which makes the same displacement field as that under a dynamic load at an arbitrary time of dynamic analysis. According to the general vibration theory associated with the finite element method (FEM), the structural dynamic behavior is presented by the following differential equation:

$$\mathbf{M}(\mathbf{b})\ddot{\mathbf{d}}(t)+\mathbf{K}(\mathbf{b})\mathbf{d}(t)=\mathbf{f}(t)=\{0\cdots 0\ \ f_i\cdots f_{i+l-1}\ \ 0\cdots 0\}^{\mathrm{T}} \tag{2-1}$$

where **M** is the mass matrix; **K** is the stiffness matrix; **f** is the vector of external dynamic

loads; **d** is the vector of dynamic displacements; and l is the number of non-zero components of the dynamic load vector. The static analysis with the FEM formulation is expressed as

$$\mathbf{K}(\mathbf{b})\mathbf{x} = \mathbf{s} \tag{2-2}$$

where **x** is the vector of static displacements and **s** is the vector of external static loads. Equations (2-1) and (2-2) are modified to calculate the static load vector which generates an identical displacement field with that from a dynamic load vector at an arbitrary time t_a as following:

$$\mathbf{s} = \mathbf{K}\mathbf{d}(t_a) \tag{2-3}$$

The vector of dynamic displacement $\mathbf{d}(t_a)$ at a certain time can be obtained from Eq. (2-1). Substituting $\mathbf{d}(t_a)$ into **x** in Eq. (2-2), the equivalent static loads are represented as Eq. (2-3). The static load vector **s**, which is generated by Eq. (2-3), is an equivalent static load vector that makes the same displacement as that from the dynamic load at a certain time. The global stiffness matrix **K** in Eq. (2-3) can be obtained from the finite element model. Therefore, the equivalent static loads are calculated by multiplication of the global stiffness matrix and the vector of dynamic displacements. The calculated sets of equivalent static loads are utilized as multiple loading conditions in the optimization process.

2.2 Optimization algorithm with equivalent static loads

The optimization process with equivalent static loads consists of two parts as illustrated in Fig. 2. They are the analysis domain and the design domain. Based on the results of the analysis domain, equivalent static loads are calculated for the design domain. In the design domain, static response optimization is conducted with the equivalent static loads. The modified design is incorporated to the analysis domain. The entire optimization process iterates between the two domains until the convergence criteria are satisfied. The circulative procedure between the two domains is defined as the design cycle. The design cycle is performed iteratively. Figure 3 shows the optimization process using equivalent static loads and the steps of the algorithm are as follows:

Step 1. Set $p = 0$, $\mathbf{b}_p = \mathbf{b}_0$.

Step 2. Perform transient analysis in Eq. (2-1) with $\mathbf{b}_p$ for $\mathbf{b}$ (in the analysis domain).

Step 3. Calculate the equivalent static load sets at all time steps by using Eq. (2-3).

Step 4. When $p = 0$, go to Step 5.

When $p > 0$, if $\sum_{i=1}^{q} \left\| \mathbf{f}_{eq}^{i}(p) - \mathbf{f}_{eq}^{i}(p-1) \right\| < \varepsilon$, then terminate.

Otherwise, go to Step 5. $\mathbf{f}_{eq}^{i}(p)$ is the equivalent static load vector at the ith time step and the pth iteration. ε is a very small value.

Step 5. Solve the following static structural optimization problem using various

equivalent static loads (in the design domain):

$$
\begin{aligned}
&\text{Find} && \mathbf{b} \\
&\text{to minimize} && F(\mathbf{b}) \\
&\text{subject to} && \mathbf{K}(\mathbf{b})\mathbf{x}_i = \mathbf{f}_{eq}^{i} \qquad (2\text{-}4) \\
& && (i=1, \ldots, \text{no. of time steps}) \\
& && \Phi(\mathbf{b}, \mathbf{x})_j \le 0 \\
& && (j=1, \ldots, \text{no. of constraints})
\end{aligned}
$$

where $\mathbf{f}_{eq}$ is the equivalent static load vector. It is utilized as multiple loading conditions for structural optimization.

Step 6. Set $p=p+1$, and go to Step 2.

3 Analysis of the joined-wing

3.1 Finite element model of the joined-wing

Figure 4 shows a finite element model of the joined-wing. The length from the wing-tip to the wing-root is 38 meters and the length of the chord is 2.5 meters. The model is composed of 3027 elements which have 2857 quadratic elements, 156 triangular elements and 14 rigid elements. Rigid elements make connections between the nodes of the aft-wing root with the center node of the aft-wing root. The structure has two kinds of aluminum materials. One has the Young's modulus of 72.4GPa, the shear modulus of 27.6GPa and the density 2770kg/m^3. The other has 36.2GPa, 13.8GPa and 2770kg/m^3, respectively. [3]

3.2 Loading conditions of the joined-wing

Loading conditions for structural optimization are explained. They have been defined by the AFRL. [3] Loading conditions are briefly shown in Table 1. There are 11 loading conditions which are composed of 7 maneuver loads, 2 gust loads, 1 take-off load and 1

landing load.

Gust is the movement of the air in turbulence and the gust load has a large impact on the airplane. Therefore, the gust load is the most important loading condition when an airplane wing is designed. [19-22] Static loads for the gust can be generated from an aeroelastic model which uses the Panel method. In Reference 3, the generated static loads are utilized for the design of the joined-wing. The real gust load acts dynamically on the airplane. Also, dynamic loads are required for optimization with equivalent static loads. Therefore, the static gust loads of Reference 3 are transformed to dynamic loads since generating exact dynamic loads is difficult. If there is an exact dynamic gust load, it can be directly used without the transformation process introduced here.

Generally, there are several methods for generating dynamic gust loads.[23-26] Here, the approximated dynamic load is evaluated by multiplying the static load by the α(1-cosine) function. The coefficient α is a constant. It is multiplied to a dynamic load to make the dynamic load generate the same displacements at the wing tip as the ones by static gust loads. The process to obtain the dynamic gust load is explained in the next paragraph.

Static analysis is performed to calculate the deflection of the wing tip by using a static gust load. And the maximum deflection is obtained by performing transient analysis using a dynamic load. The dynamic load is made by multiplying the static load by the α(1-cosine) function.

The duration time of the dynamic gust load is calculated from the following equation. [19]

$$U = \frac{U_{de}}{2}\left(1 - \cos\frac{2\pi s}{25C}\right) \tag{3-1}$$

Then U is the velocity of the gust load, U_{de} is the maximum velocity of the gust load, s is the distance penetrated into the gust and C is the geometric mean chord of the wing. The conditions for the coefficients are shown in Table 2. From Table 2 and Eq. (3-1), the duration time is 0.374 seconds. The airplane stays in the gust for 0.374 seconds.

The dynamic gust load is calculated from Eq. (3-2).

$$F_{dynamic} = \alpha \times \left(1 - \cos\frac{2\pi}{0.374}t\right) \times F_{static} \tag{3-2}$$

where F_{static} is the static gust load which is the eighth or ninth load in Table 1. It is noted that the period of the gust load is 0.374 second and the duration time of the dynamic load is 0.374 second. The dynamic load is 0 after 0.374 second.

The process to obtain α is explained. When loads are imposed on the joined-wing, the maximum displacement occurs at the tip. First, the tip displacement is evaluated by the first gust load (the eighth load in Table 1). A dynamic analysis is performed by the dynamic load in Eq. (3-2) with $\alpha = 1$. The maximum displacement of the dynamic analysis is compared with the static tip displacement. α is the ratio of the two displacements since the two analyses are linear problems. α is evaluated for the second gust load (the ninth load of Table 1) as well. Therefore, two dynamic load sets are made.

The following process is carried out for each dynamic gust load. Transient analysis is

performed and equivalent static loads are generated. Results of the transient analysis are illustrated in Fig. 5. The tip of the wing vibrates. As illustrated in Fig. 5, the maximum displacement of the wing tip occurs after 0.374 second, which is the duration time of the dynamic load. Also, the maximum displacement occurs within 3 seconds. The duration time is set by 3 seconds and the duration is divided into 100 time steps. Therefore, 200 sets of equivalent static loads are generated from the two dynamic gust load cases. The number of the other static loads is 9 in Table 1. Nine kinds of the static loads are maneuver, taxing and landing load. Therefore, the number of the total load cases is 209, which consists of 9 static loads and 200 equivalent static loads. 209 static loading conditions are utilized as multiple loading conditions in the optimization process.

3.3 Boundary conditions of the joined-wing

As illustrated in Fig. 4, the fore-wing and the aft-wing are joined together in the joined-wing. Since the root of the fore-wing is attached to the fuselage, all the degrees of freedom of the six directions are fixed. The six directions are x, y, z-axis translational directions and x, y, z-axis rotational directions. It is presented in Fig. 6. The aft-wing is also attached to the fuselage at the boundary nodes and the center node as illustrated in Fig. 6. The center node has an enforced rotation with respect to the y-axis. Each load in Table 1 has a different amount of enforced rotation. The enforced rotation generates torsion on the aft-wing and has quite an important aerodynamic effect. The amounts of

the enforced rotation are from -0.0897 radian to 0 radian.[3] The boundary nodes are set free in x and z translational directions. Other degrees of freedom are fixed. The boundary conditions are illustrated in Fig. 6.

4 Structural optimization of the joined-wing

4.1 Definition of design variables

As mentioned earlier, the FEM model has 3027 elements. It is not reasonable to select the properties of all the elements as design variables for optimization. Thus, the design variable linking technology is utilized. The wing structure is divided into 48 sections and each section has the same thickness. The finite element model is adopted from Reference 3. The model in Reference 3 has a different thickness for 3027 elements. Therefore, each thickness of the 48 sections is made by the average of the element thicknesses in a section. The average value of each section is utilized as the initial design in the optimization process.

First, the joined-wing is divided into 5 parts, which are the fore-wing, the aft-wing, the mid-wing, the wing tip and the edge around the joined-wing. The parts are illustrated in Fig. 7. Each part is composed of the top skin, the bottom skin, the spar and the rib. The top and bottom skins are divided into three sections. Only 43 sections among the 48 sections are used as design variables. Figure 8 presents the division for the mid-wing. Other parts such as the fore-wing, the aft-wing, the wing tip and the edge are divided in the same manner. The spar of the tip wing and the top skin, the bottom skin and the rib of the

edge part are not used as design variables. Design variables are defined based on the Reference 3.

4.2 Formulation

The formulation for optimization is

$$\begin{aligned} &\text{Find} && t_i \quad (i = 1, \cdots, 43) \\ &\text{to minimize} && \text{Mass} \\ &\text{subject to} && |\sigma_j| \le \sigma_{allowable} \quad (j = 1, \cdots, 2559) \\ & && 0.001016\text{m} \le t_i \le 0.3\text{m} \quad (i = 1, \cdots, 43) \end{aligned} \tag{4-1}$$

The initial model in Reference 3 has 3027 elements and each element has a different thickness. The mass of the initial model is 4199.7kg. Static response optimization is carried out for the initial model. As mentioned earlier, the initial model is divided into 48 sections, the initial thickness is defined by the average value. Then, the mass of this modified model is 4468.6kg. This model is utilized in static response optimization and dynamic response optimization using equivalent static loads.

The material of the joined-wing is aluminum. The allowable von Mises stress for aluminum is set by 253MPa. Since the safety factor 1.5 is used, the allowable stress is reduced to 169MPa. [3] Stresses of all the elements except for the edge part should be less

than the allowable stress, 169MPa. Lower and upper bounds of the design variables are set by 0.001016m and 0.3m, respectively.

5 Results and discussion

5.1 Optimization results

The results from dynamic response optimization with equivalent static loads are compared with the results from static response optimization. Static response optimization is performed for two cases with different definitions of design variables. CASE 1 and CASE 2 are static response optimization and CASE 3 is dynamic response optimization.

CASE 1 is the static response optimization with the 11 loads in Table 1. In the model of CASE, 1 the thickness of all elements is different and the starting mass is 4199.7kg. Design variables are thicknesses of the structure except for the edge part of the joined-wing. The number of design variables is 2559. Constraints are imposed on the stresses as Eq. (4-1). Table 3 and Fig. 9 show the results of optimization. Constraint violation in Table 3 is the value when static response optimization is performed. The value in the parenthesis is the one when transient analysis is performed with the design. As shown in Table 3, the constraints are satisfied in the static response optimization process. But when transient analysis is performed with the optimum solution, it is noted that the constraints are violated. That is, static response optimization is not sufficient for a dynamic system. The static response optimization process converges in 24 iterations and the CPU is 29

hours and 30 minutes with an HP Unix Itanium 1.6GHz CPU 4. The objective function increases about 13.2 percent from 4199.7kg to 4755.1kg. The commercial software called GENESIS is utilized for the optimization process. [17] Transient analysis is performed by NASTRAN. [18]

CASE 2 is performed under the same loading condition as CASE 1. The model for CASE 2 has 48 sections. The starting value of the mass is 4468.6kg. The loading conditions are the same as those of CASE 1. The formulation of the optimization process is shown in Eq. (4-1). As mentioned earlier, there are 43 design variables. The history of the optimization process is shown in Table 4 and Fig. 10. Constraint violation in Table 4 is expressed in the same way as Table 3. In CASE 2, the constraints are satisfied in the optimization process. When transient analysis is performed with the optimum solution, the stress constraints are violated. The process converges in four iterations and the CPU time is 30 minutes. The mass increases about 144 percent from 4468.6kg to 10901.66kg. The commercial software for the optimization process is NASTRAN [18] and the computer is an AMD Athlon 64bit Processor, 2.01GHz, 1.0GB RAM.

CASE 3 uses dynamic response optimization. The dynamic loads are the ones explained in Section 3.2. The design variables are the same as those of CASE 2. Dynamic loads are made for the two gust loads in Table 1 and equivalent static loads are generated. As explained in Section 3.2, 209 loading conditions are used in a static response optimization process. The model of CASE 3 is equal to the model of CASE 2. The process converges in 10 cycles. One cycle is a process between the analysis domain

and the design domain. The total CPU time is 21 hours and 10 minutes. As shown in Table 5, the mass of the joined-wing is increased by 184.8 percent from the initial mass. It is noted that the constraints are satisfied when transient analysis is performed with the optimum solution. Then commercial software system and the computer used for the optimization process are the same as the ones of CASE 2.

5.2 Discussion

Figure 12 shows the results of design variables from CASE 1. Part A in Fig. 9 has the lower bound and the optimum values of part B are larger than 1cm. Generally, the wing tip has the lower bound and the thickness of the aft-wing is larger than that of the fore-wing.

The results of the top and bottom skins of the aft-wing are illustrated in Fig. 13 for CASE 2 and CASE 3. The thicknesses of the skins of the aft-wing become larger compared to the initial thicknesses. The parts A and B of the top skin in Fig. 13 have thicknesses three times larger than that of CASE 2. Also, part C has four times larger thickness.

The changes of the spar of the aft-wing are shown in Fig. 14. In A of Fig. 14, the optimum thickness of CASE 2 is 2.3 times larger than that of CASE 3. The results of the two cases are similar for B in Fig. 14. The thickness of part C becomes larger than the initial thickness in CASE 2, but it is reduced by 70% in CASE 3. Fig. 15 shows the

results of the design variables at the top and bottom skins of the fore-wing. Figure 16 shows the results at the spar of the mid-wing. It is noted that the results of static response optimization and dynamic response optimization are considerably different.

Transient analysis with optimum solutions is performed for the three cases to verify the optimization results. Stress distribution of each case is shown in Figs. 17-19 when the maximum stress occurs. As shown in Fig. 14, the maximum stress of CASE 1 occurs at the top skin of the fore-wing. The magnitude of the stress is 490MPa and it occurs at the time of 1.17 seconds. The stress contour for CASE 2 is illustrated in Fig. 15. The maximum stress is 253MPa at the top skin of the aft-wing root at the time of 2.55 seconds. Figure 19 is for CASE 3. The maximum stress occurs at the time of 1.26 seconds and it is 170MPa at the top skin of the mid-wing.

The maximum stresses of the three cases have different magnitudes and locations. When transient analysis is performed, constraints are violated in CASE 1 and CASE 2 while they are satisfied in CASE 3. Therefore, optimization with equivalent static loads accommodates the dynamic characteristics quite well.

6 Conclusions

A joined-wing which has a longer range and loiter than a conventional wing is investigated from the viewpoint of weight reduction. Structural optimization considering dynamic effect is required due to the characteristics of the aircraft which must endure dynamic loads. Especially, gust loads should be considered in the design of the aircraft. Calculating exact dynamic gust load is difficult in that complicated aeroelastic analysis is required. Therefore, approximated dynamic gust loads are evaluated using an approximation method. The function (1-cosine) is used for the approximation. Structural optimization is performed for mass reduction by using equivalent static loads. An equivalent static load is a static load which makes the same displacement field as that under a dynamic load at an arbitrary time. The equivalent static load can consider the exact dynamic effect compared to the conventional dynamic factors.

When transient analysis is performed, it is found that the maximum stress of the initial design is three times of the allowable stress. Static response optimization is carried out based on the given loads. When transient analysis is performed with the optimum solution of static response optimization, the constraint is violated by 50 %. However, the optimization results with equivalent static loads satisfy the constraints. It is found that the equivalent static loads accommodate the dynamic effect very well.

The dynamic load for the equivalent static loads is calculated by using the approximation method of the (1-cosine) function. In the future, it will be necessary to generate exact dynamic loads by using aeroelastic analysis. Also, the deformation of the joined-wing is considerably large in the elastic range. It has geometric nonlinearity. The fully stressed design algorithm has been used with nonlinear static analysis of the joined-wing. [3] It will be necessary to perform structural optimization considering the nonlinearity of the joined-wing using equivalent static loads.

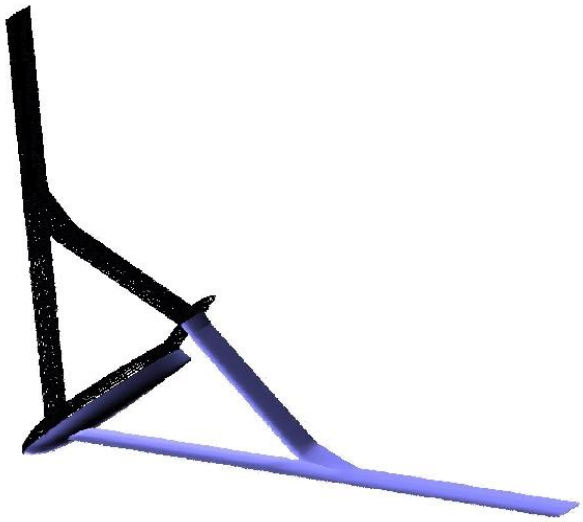

Fig. 1 Configuration of the joined-wing

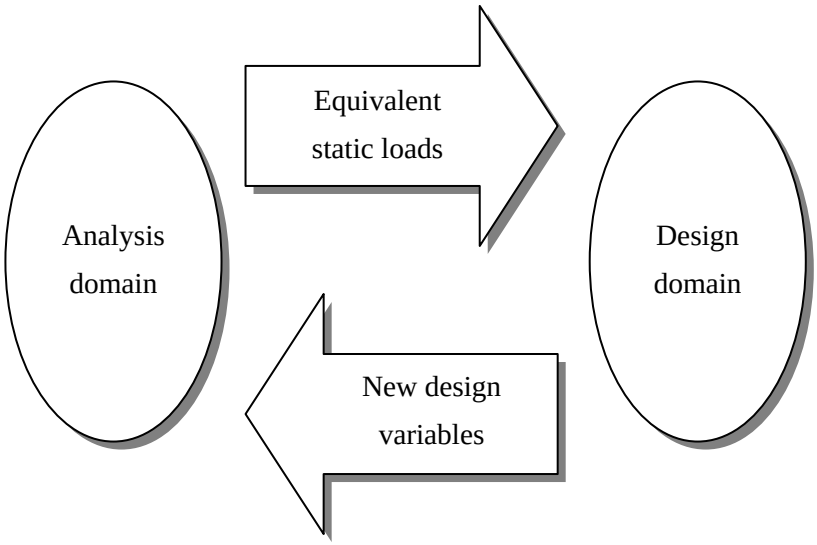

Fig. 2 Schematic process between the analysis domain and the design domain

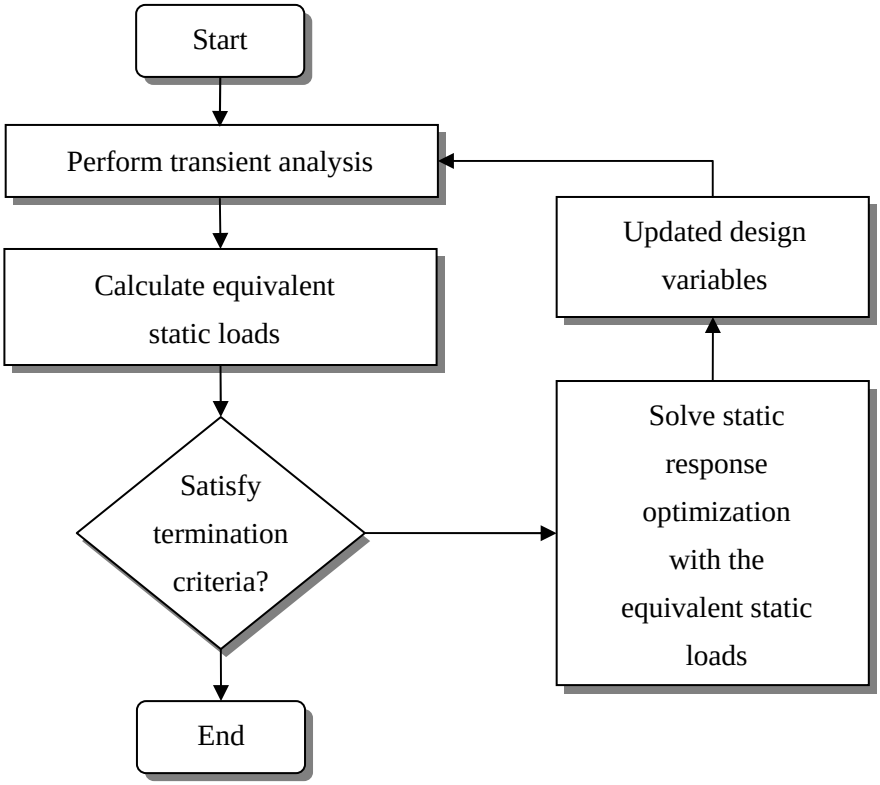

Fig. 3 Optimization process using equivalent static loads

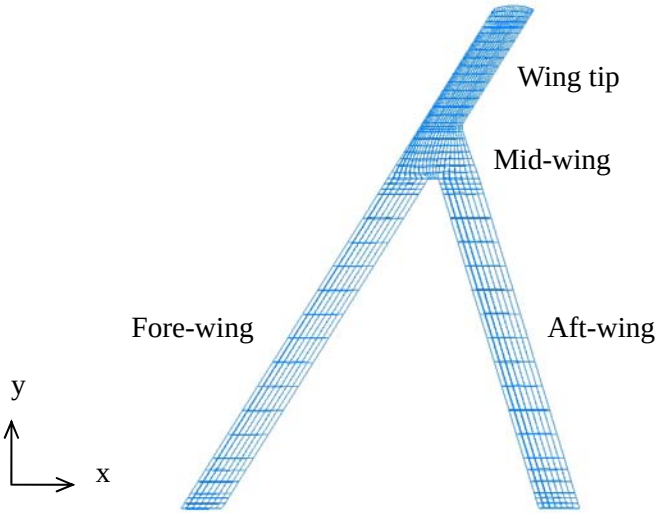

Fig. 4 Finite element modeling of the joined-wing

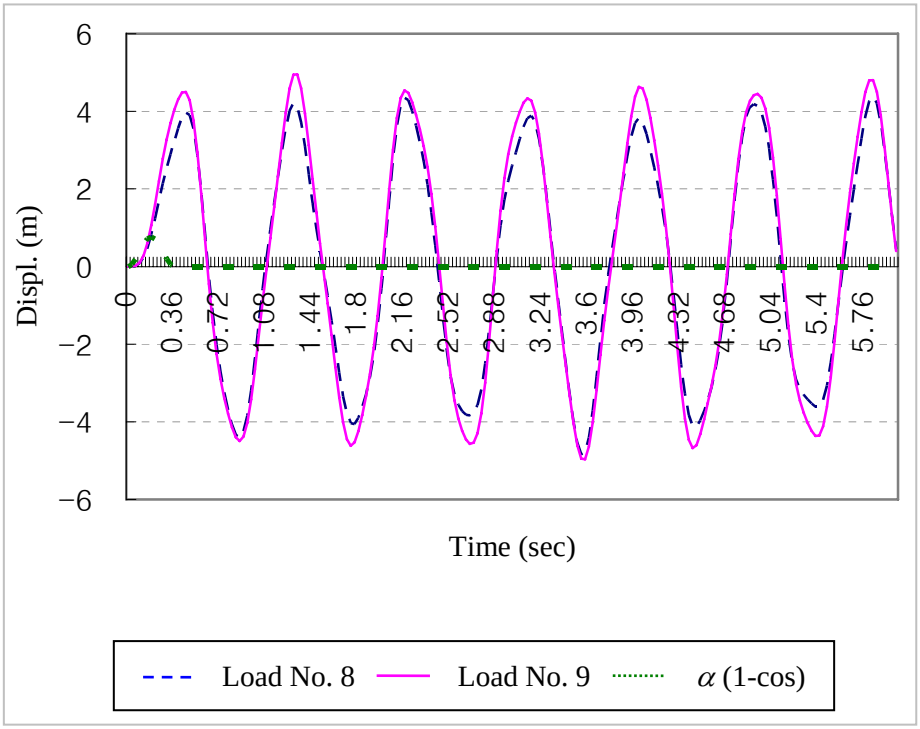

Fig. 5 Vibration of the wing tip deflection

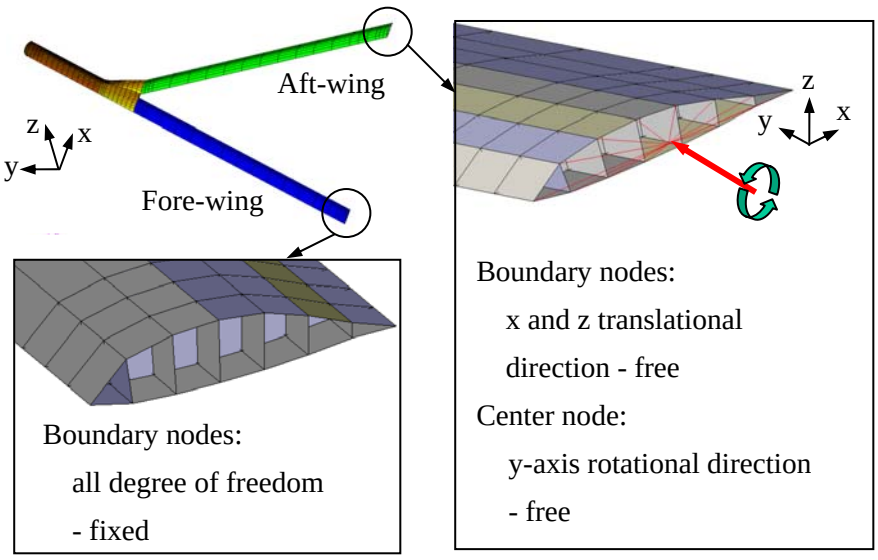

Fig. 6 Boundary conditions of the joined-wing

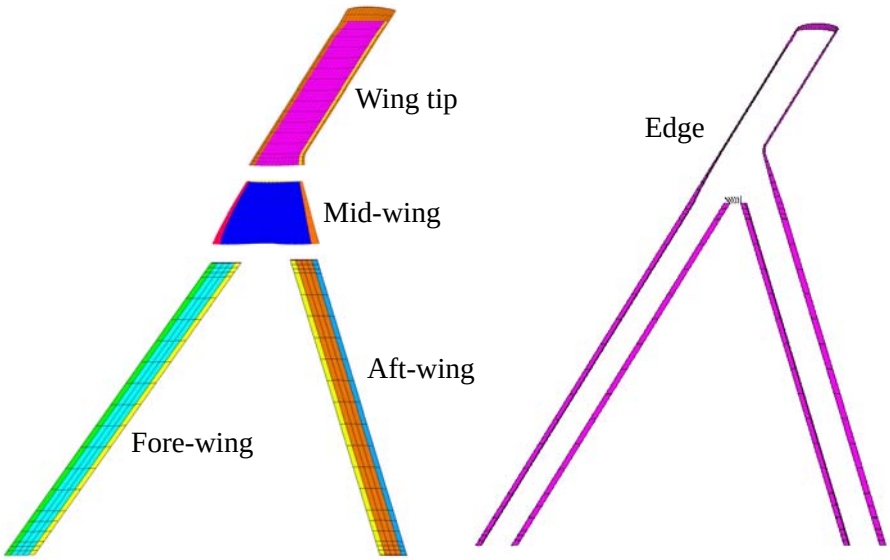

Fig. 7 Five parts for definition of design variables

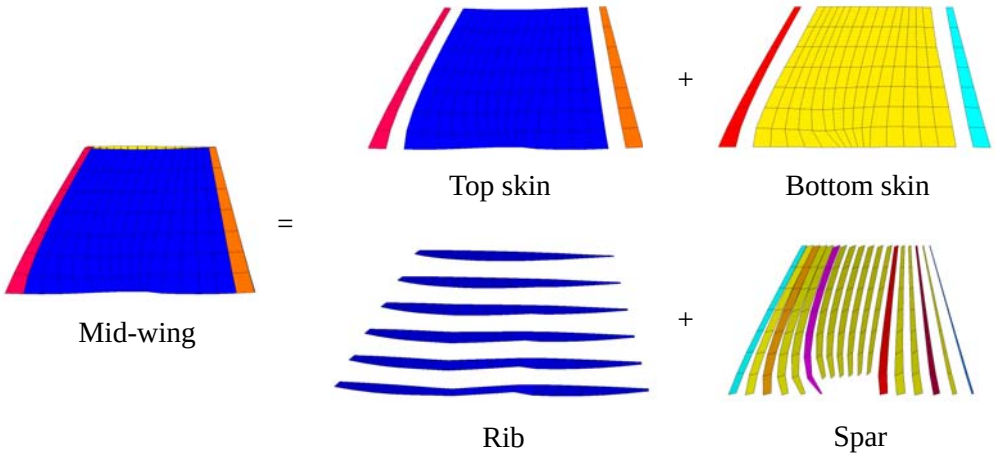

Fig. 8 Sections for definition of design variables

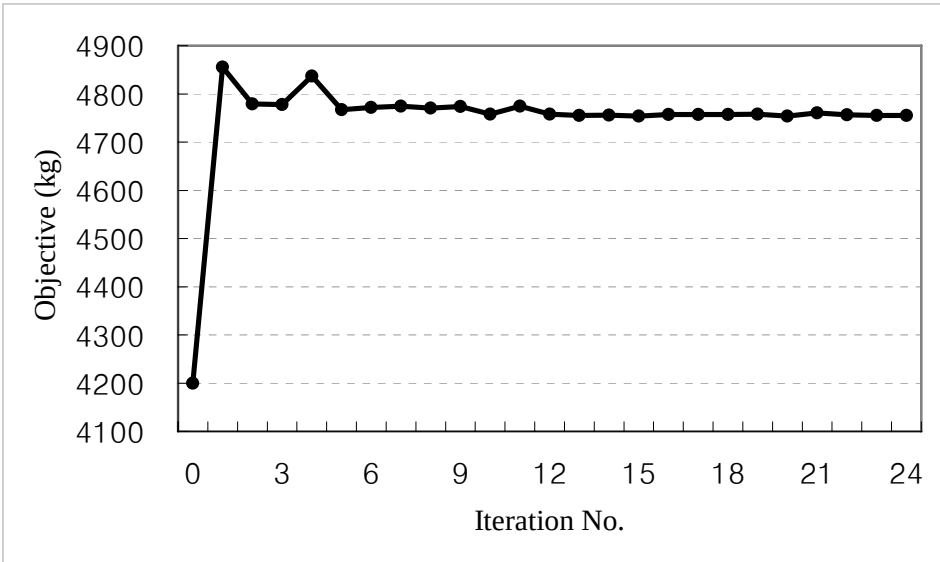

Fig. 9 The history of the objective function of CASE 1

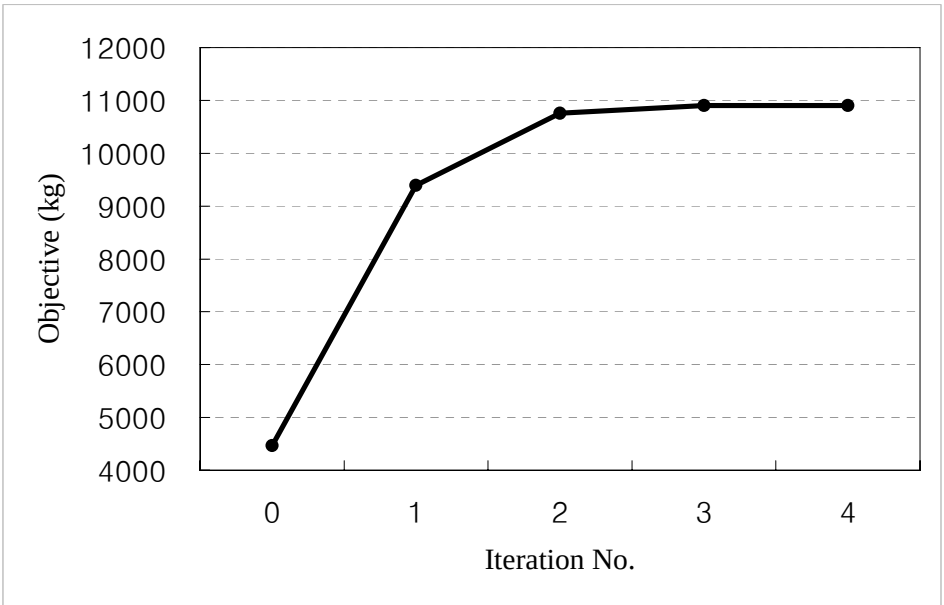

Fig. 10 The history of the objective function of CASE 2

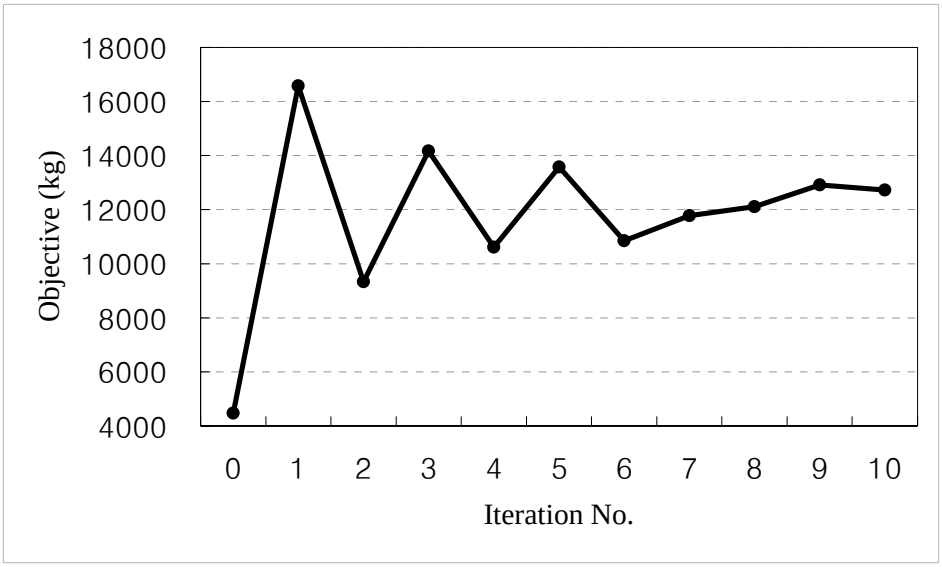

Fig. 11 The history of the objective function of CASE 3

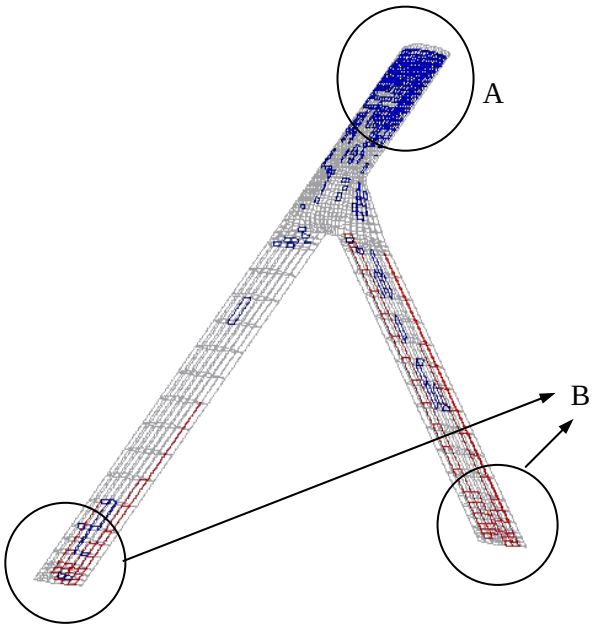

Fig. 12 Results of the design variables of CASE 1

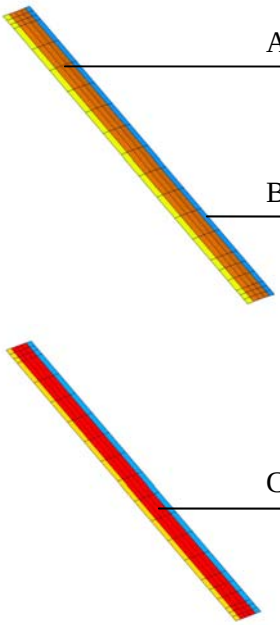

A

Initial (m)	CASE 2 (m)	CASE 3 (m)
0.002718	0.009081	0.029016

B

Initial (m)	CASE 2 (m)	CASE 3 (m)
0.001493	0.003470	0.009377

C

Initial (m)	CASE 2 (m)	CASE 3 (m)
0.001554	0.006884	0.027157

Fig. 13 Results of the design variables at the skin of the aft-wing

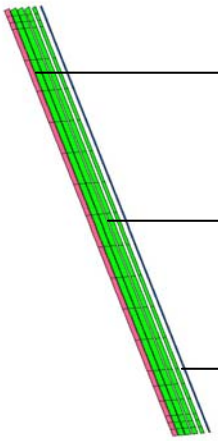

A

Initial (m)	CASE 2 (m)	CASE 3 (m)
0.001016	0.005682	0.002494

B

Initial (m)	CASE 2 (m)	CASE 3 (m)
0.001016	0.003736	0.003742

C

Initial (m)	CASE 2 (m)	CASE 3 (m)
0.0825	0.107	0.02329

Fig. 14 Results of the design variables at the spar of the aft-wing

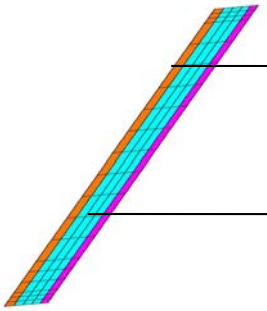

Initial (m)	CASE 2 (m)	CASE 3 (m)
0.002578	0.01072	0.011126

Initial (m)	CASE 2 (m)	CASE 3 (m)
0.004656	0.015514	0.011862

Initial (m)	CASE 2 (m)	CASE 3 (m)
0.009598	0.034552	0.024566

Fig. 15 Results of the design variables at the skin of the fore-wing

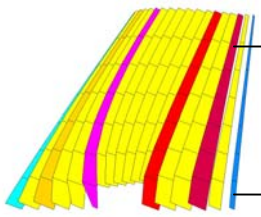

Initial (m)	CASE 2 (m)	CASE 3 (m)
0.001016	0.006283	0.004891

Initial (m)	CASE 2 (m)	CASE 3 (m)
0.001016	0.003934	0.002331

Fig. 16 Results of the design variables at the spar of the mid-wing

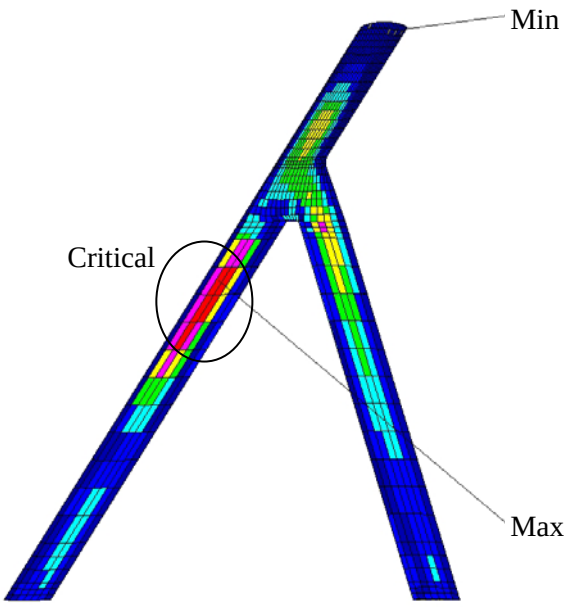

Fig. 17 Stress contour of CASE 1

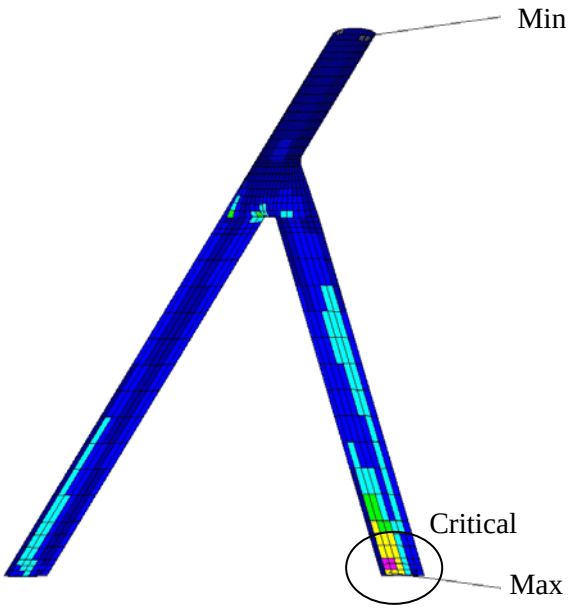

Fig. 18 Stress contour of CASE 2

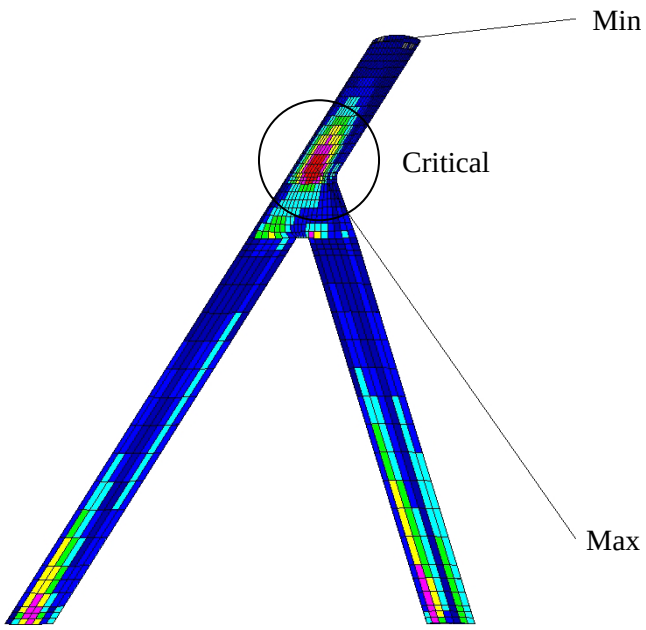

Fig. 19 Stress contour of CASE 3

Table 1 Loading conditions for optimization

Load No.	Load Type	Mission Leg
1	2.5g PullUp	Ingress
2	2.5g PullUp	Ingress
3	2.5g PullUp	Loiter
4	2.5g PullUp	Loiter
5	2.5g PullUp	Egress
6	2.5g PullUp	Egress
7	2.5g PullUp	Egress
8	Gust (Maneuver)	Descent
9	Gust (Cruise)	Descent
10	Taxi (1.75g impact)	Take-Off
11	Impact (3.0g landing)	Landing

Table 2 Aerodynamic data for the joined-wing

Gust maximum velocity	18.2m/s
Flight velocity	167m/s
Geometric mean chord of wing	2.5m
Distance penetrated into gust	62.5m

Table 3 Results of the objective and constraint functions for CASE 1

Iteration No.	Optimum Value (kg)	Constraint Violation (%)
0	4199.7	142.1 (216.009)
1	4855.8	68.4
2	4778.9	105.5
3	4777.5	47.4
4	4837.0	26.4
5	4767.1	41.7
6	4771.9	31.8
…	…	…
18	4757.4	16.8
19	4758.1	10.7
20	4754.1	2.8
21	4760.5	1.6
22	4756.6	2.8
23	4755.2	0.5
24	4755.1	0.3 (190.307)

Table 4 Results of the objective and constraint functions for CASE 2

Iteration No.	Optimum Value (kg)	Constraint Violation (%)
0	4468.60	173.829(344.213)
1	9391.202	25.055
2	10759.24	0.600
3	10901.66	0.204
4	10901.66	0.204(49.561)

Table 5 Results of the objective and constraint functions for CASE 3

Iteration No.	Optimum Value (kg)	Constraint Violation (%)
0	4468.60	344.213
1	16527.18	-16.427
2	9329.58	40.759
3	14172.92	66.899
4	10610.69	23.755
5	13579.97	18.89
6	10852.17	14.993
7	11782.34	6.196
8	12112.68	8.368
9	12918.26	1.26
10	12725.52	0.681

References

1. J. Wolkovich, 1986, “The Joined-Wing: An Overview,” Journal of Aircraft, Vol. 23, No. 3, pp. 161-178.
2. J.W. Gallman and I.M. Kroo, 1996, “Structural Optimization of Joined-Wing Synthesis,” Journal of Aircraft, Vol. 33, No. 1, pp. 214-223.
3. M. Blair, R.A. Canfield and R.W. Roberts, 2005, “Joined-Wing Aeroelastic Design with Geometric Nonlinearity,” Journal of Aircraft, Vol. 42, No. 4, pp. 832-848.
4. M. Blair and R.A. Canfield, 2002, “A Joined-Wing Structural Weight Modeling Study,” 45th AIAA/ASME/ASCE/AHS/ASC Structures, Structural Dynamics and Materials Conference, Denver, CO, USA.
5. R.W. Roberts, R.A. Canfield and M. Blair, 2003, “Sensor-Craft Structural Optimization and Analytical Certification,” 44th AIAA/ASME/ASCE/AHS/ASC Structures, Structural Dynamics and Materials Conference, Norfolk, VA, USA.
6. C.C Rasmussen, R.A. Canfield and M. Blair, 2004, “Joined-Wing Sensor-Craft Configuration Design,” 45th AIAA/ASME/AHS/ASC Structures, Structural Dynamics and Materials Conference, Palm Springs, CA, USA.
7. C.C Rasmussen, R.A. Canfield and M. Blair, 2004, “Optimization Process for Configuration of Flexible Joined-Wing,” 10th AIAA/ISSMO Multidisciplinary Analysis and Optimization Conference, Albany, NY, USA.
8. B.S. Kang, G.J. Park, J.S. Arora, 2005, “A Review of Optimization of Structures Subjected to Transient Loads,” Structural and Multidisciplinary Optimization (accepted).
9. W.S. Choi and G.J. Park, 1999, “Transformation of Dynamic Loads into Equivalent Static Loads Based on Model Analysis,” International Journal for Numerical Methods in Engineering, Vol. 46, No. 1, pp. 29-43.
10. W.S. Choi and G.J. Park, 2000, “Quasi-Static Structural Optimization Technique Using Equivalent Static Loads Calculated at Every Time Step as a Multiple Loading Condition,” Transactions of the Korean Society of Mechanical Engineers (A), Vol. 24, No. 10, pp. 2568-2580.
11. W.S. Choi and G.J. Park, 2002, “Structural Optimization Using Equivalent Static Loads at All the Time Intervals,” Computer Methods in Applied Mechanics and

Engineering, Vol. 191, No. 19, pp. 2077-2094.
12. B.S. Kang, W.S. Choi and G.J. Park, 2003, “Structural Optimization Under Equivalent Static Loads Transformed from Dynamic Loads Based on Displacement,” Computers & Structures, Vol. 79, pp. 145-154.
13. G.J. Park and B.S. Kang, 2003, “Mathematical Proof for Structural Optimization with Equivalent Static Loads Transformed from Dynamic Loads,” Transactions of the Korean Society of Mechanical Engineers (A), Vol. 27, No. 2, pp. 268-275.
14. G.J. Park and B.S. Kang, 2003, “Validation of a Structural Optimization Algorithm Transforming Dynamic Loads into Equivalent Static Loads,” Journal of Optimization Theory and Applications, Vol. 118, No. 1, pp. 191-200.
15. K.J. Park, J.N. Lee and G.J. Park, 2005, “Structural Shape Optimization Using Equivalent Static Loads Transformed from Dynamic Loads,” International Journal for Numerical Methods in Engineering, Vol. 63, No. 4, pp. 589-602.
16. B.S. Kang, G.J. Park and J.S. Arora, 2005, “Optimization of Flexible Multibody Dynamic Systems Using the Equivalent Static Load,” Journal of American Institute Aeronautics and Astronautics, Vol. 43, No. 4, pp. 846-852.
17. GENESIS User’s Manual: Version 7.0, 2001, Vanderplaats Research and Development, Inc.
18. MSC.NASTRAN 2004 Reference Manual, 2003, MSC. Software Corporation.
19. F.M. Hoblit, 1988, Gust Loads on Aircraft: Concepts and Applications, American Institute of Aeronautics and Astronautics, Inc., Washington, D.C.
20. T.H.G. Megson, 1999, Aircraft Structures, Engineering students third edition, Butterworth Heinemann, London, U.K.
21. A. Kareem and Y. Zhou, 2003, “Gust Loading Factor-Past, Present and Future,” Journal of Wind Engineering and Industrial Aerodynamics, Vol. 91, No. 12/15, pp. 1301-1328.
22. T.C. Corke, 2002, Design of Aircraft, Prentice Hall, NJ, USA.
23. S.S. Rao, 1985, “Optimization of Airplane Wing Structures Under Gust Loads,” Computers & Structures, Vol. 21, No. 4, pp. 741-749.
24. R. Noback, 1986, “Comparison of Discrete and Continuous Gust Methods for Airplane Design Loads Determination,” Journal of Aircraft, Vol. 23, No. 3, pp. 226-231.

25. J.R. Fuller, 1995, “Evolution of Airplane Gust Loads Design Requirements,” Journal of Aircraft, Vol. 32, No. 2, pp. 235-246.
26. R. Singh and J.D. Baeder, 1997, “Generalized Moving Gust Response Using CFD with Application to Airfoil-Vortex Interaction,” 15th AIAA Applied Aerodynamics Conference, Atlanta, GA, USA.